Available online at www.sciencedirect.com

ScienceDirect

Mendeleev Commun., 2020, **30**, 809–811

Mendeleev Communications

Formation of hollow silica spheres from molecular silica sols

Kirill M. Borisov,[a,b,c] Elena S. Bokova,[c] Alexandra A. Kalinina,[a,b] Evgeniya A. Svidchenko,[a] Aleksandra V. Bystrova,[a,b] Anastasiya M. Sumina,[d] Martin Moeller[b] and Aziz M. Muzafarov*[a,b]

[a] *N. S. Enikolopov Institute of Synthetic Polymeric Materials, Russian Academy of Sciences, 117393 Moscow, Russian Federation. Fax: +7 495 718 3404; e-mail: aziz@ispm.ru*

[b] *A. N. Nesmeyanov Institute of Organoelement Compounds, Russian Academy of Sciences, 119991 Moscow, Russian Federation. Fax: +7 499 135 6549*

[c] *A. N. Kosygin Russian State University, 115035 Moscow, Russian Federation*

[d] *M. M. Shemyakin–Yu. A. Ovchinnikov Institute of Bioorganic Chemistry, Russian Academy of Sciences, 117997 Moscow, Russian Federation*

DOI: 10.1016/j.mencom.2020.11.040

Hollow silica microspheres have been obtained in a surfactant-free templating process at neutral pH from silica sol of 2–10 nm globular organic–inorganic silica particles with exposed hydrophobic siloxane part as well as hydrophilic reactive silanol groups. Due to small diffusion coefficient and amphiphilic nature, the sol particles stabilize an oil–water interface quickly. Initially they assemble *via* noncovalent interaction into a stable shell and then condense covalently, with fast initial stabilization/dispersion of oil–water emulsion improving the control and simplifying the microsphere formation process.

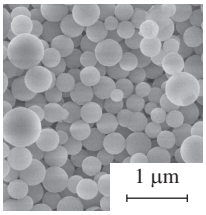

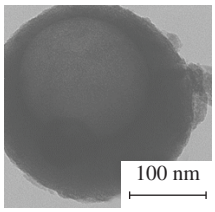

Keywords: silica microcapsules, molecular silica sol, Pickering emulsion, encapsulation, microspheres.

Hollow micro- and nanostructures such as microspheres have high potential for their use in a number of technological processes associated with light-weight materials,[1] modulation of refractive index,[2,3] compensation of cyclic thermal expansion,[4] *e.g.*, in lithium-ion batteries,[5] as well as for thermal insulation coatings.[6,7] Furthermore, the voids within these structures can be loaded with functional components such as drugs.[8,9] For a survey of synthetic strategies for their preparation, we refer to the notable reviews.[10,11]

Within the class of hollow structures, the materials composed of silica play a dominant role, last not least because of their versatile fabrication methods and biocompatibility. Advantages of silica as the wall forming material comprise its stiffness, porosity and simple chemical modification by organosilanes.[12,13] Also, the thickness of the shell can be tailored according to desirable mechanical strength, flexibility and the minimum volume fraction.[14–17] Bioresorption and non-toxicity provide further unique selling points as well.[18–20]

Two methods are typically used for fabrication of hollow microspheres from silica or organosilicon compounds. The first one implies formation of colloidosomes when solid silica nanoparticles are adsorbed at an oil–water phase boundary to form solid-stabilized or Pickering emulsion.[21–25] This way, water-in-oil as well as oil-in-water emulsions can be employed.[26] Hyperbranched polyethoxysiloxane (PEOS) acts as a binder for the particles to build the silica colloidosomes with tunable characteristics.[25,27–29] The second approach represents emulsion templating[14] based on the use of surfactants. A silica precursor such as tetraethoxysilane (TEOS) is added to an oil-in-water emulsion or an inverse one. Droplets of the minor phase serve as templates as the silica precursor gets adsorbed at the oil–water interface and undergoes hydrolysis to yield a solid shell. Note that this technique allows the formation of regular mesoporous shell structures if the surfactant employed is able to form a mesophase structure within the solidifying silica layer.[30,31] However, formation of small spheres typically requires significant amount of the surfactant. An exception represents the formation of silicone–silica hybrid colloids in a two-step procedure from dimethyldiethoxysilane (DMDES) as a precursor.[14] Initially, an oil-in-water emulsion is prepared by hydrolysis and polymerization of DMDES, then the silicone droplets are covered by a silica layer formed from TEOS at high pH. After the core removal, rather uniform hollow silica spheres are formed with a diameter of ~500 nm, and their elasticity can be tailored by the thickness of the wall, *i.e.*, the amount of TEOS employed. Yet, the examples are limited to the combination of TEOS–DMDES and the core removal requires an extensive extraction.[14] One more surfactant-based approach avoids the use of oil droplets as a template for the hollow shell structures and employs vesicular surfactant assemblies, whereby a hydrophobic silicon alkoxide precursor is hydrolyzed within the interlayered regions of multilamellar surfactant vesicles.[32]

Using the above Pickering approach, a contamination by surfactant can be avoided and rather stable spheres are produced. However, their diameter cannot be lowered to the submicron level, and an energy-intensive shearing is indispensable. On the other hand, employing the emulsion templating makes necessary a thorough purification from surfactants before further application. Hence, the development of surfactant-free syntheses of functional submicron hollow spheres is of certain interest.

In this work, we used silica sol with surface-reactive silica particles as a precursor for the shell of microspheres. The ultrasmall particles with diameter below 2–3 nm combine the features of Pickering and surfactant-based stabilization types of

an emulsion. It is known, that the adsorption energy E of a colloid at an oil–water interface scales with the square root of the particle radius r:[33]

$$E = \pi r^2 \gamma_{o/w}(1 \pm \cos\theta)^2, \quad (1)$$

where $\gamma_{o/w}$ represents the oil–water interface tension and θ is the particle–interface contact angle, the E value being maximal at $\theta = 90°$. Only when the particle size becomes less than a few nm, the energy of detachment decreases to values below 50 kT. Since the diffusion coefficient of small particles is inversely proportional to their radius, an equilibration of size distribution and surface-to-volume ratio of the droplets becomes efficient solely for particles with a diameter less than 2–3 nm. In combination with their amphiphilic surface structure, such particles resemble fungal hydrophobins with a known unique surface activity.[34] Suitable globular hybrid organic–inorganic silica particles with diameter lower than 10 nm and down to 2 nm with exposed hydrophobic siloxane moieties as well as hydrophilic reactive silanol groups had been developed by our group in the form of silica sols in THF.[35,36] They combine structural features of ultrasmall colloids with the solubility and chemical functionality of macromolecules, as it has been well established for the globular proteins. Here we describe the ability of these silica sols to stabilize an oil-in-water emulsion and the subsequent microcapsules formation.†

In a first step, we explored the agglomeration of silica sol particles when their solution in THF was introduced into water at pH 7 and dispersed at 5×10^3 rpm to obtain solid spherical particles without internal cavities [Figure 1(*a*),(*b*)]. The electron micrographs confirmed size-controlled condensation reaction of the sol particles in the neutral aqueous solution. Formation of spheres and their size could be controlled by the concentration and mixing conditions when the THF solution was introduced into water. Hence, the condensation reaction between the silica sol particles was slow enough to allow the controlled dispersion/precipitation.

In a second series of experiments, the THF–silica sol was added to a heavily stirred dispersion of toluene or D_4 as a hydrophobic liquid. The original oil droplet size was varied by the appropriate rotation speed during emulsification (Table 1). For the efficient dispersion, it was necessary to keep the process of condensation of OH groups of molecular silica sol sufficiently slow, therefore the experiments were carried out at pH 7.

† SEM measurements were performed using an NVision 40 scanning electron microscope (Carl Zeiss) equipped with an X-Max detector (Oxford Instruments) operated at accelerating voltages of 3–20 kV. TEM measurements were carried out on a LEO912 AB OMEGA instrument (Carl Zeiss) at accelerating voltages of 60, 80, 100 and 120 kV. For confocal microscopy, an Eclipse TE-2000 inverted microscope (Nikon) was employed with a C1 confocal laser system including Kr (408), Ar (488) and G-NeHe (543 nm) lasers, samples were prepared applying 30 μl of an emulsion to the coverslips.

FTIR spectra were recorded employing a Bruker Equinox 55/S instrument.

Specific surface area was measured using the method of thermal desorption of Ar on a Tsvet-211 instrument (Russia) and then calculated according to BET theory with the Temkin equation for monolayer capacity employing the values of $P/P_0 = 0.23$, $P_b = 729$ Torr and $T = 22$ °C.

Density of the powders was determined at 20 °C in a chamber of 4 cm^3 volume using a Pycnomatic ATC gas pycnometer (Thermo Fisher Scientific).

Silica sol was prepared according to the described multistep procedure[35] as 10% colloidal solution in THF of spherical silica particles enriched with hydroxyl groups, the solution was stable due to solvation of the OH groups.[36]

For the preparation of microspheres, an oil, namely toluene or octamethylcyclotetrasiloxane (D_4), was dispersed in the water phase at pH 7 (oil–water mass ratio was 1 : 100) under stirring using a T50 ULTRA-TURRAX mechanical disperser (IKA) at definite rotation speed for 1 min. With continued stirring, the silica sol solution in THF was introduced to the emulsion at oil–SiO_2 mass ratio of 10 : 7 and the emulsification was further continued for 15 s. The product was isolated by centrifugation at 1.1×10^4 rpm for 20 min, washed with water and dried *in vacuo*.

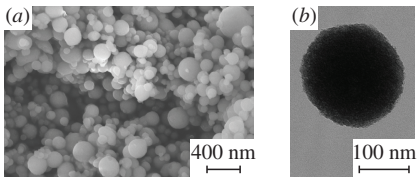

Figure 1 (*a*) SEM and (*b*) TEM images of particles prepared by dispersing the silica sol in water at 5×10^3 rpm.

Table 1 summarizes the results obtained. Whether hollow or macroporous spheres had been formed, was determined from SEM and TEM images of the dried particles. With toluene as a liquid for the hydrophobic template droplets, the hollow spheres were formed at the intermediate rotation speed value. At lower speeds, spheres with a microscopically homogeneous cross section were formed (Table 1, entry 1 as well as Figure 2). The absence of empty core is indicated by the lack of any contrast across the particles in the TEM image [Figure 2(*b*)].

Thus, templating by preferential deposition of silica sol particles at the surface of droplets did not take place. This can be rationalized if the toluene droplets are too large (*i.e.*, have small surface-to-volume ratio and long average distance apart) to favor nucleation during the shell formation at their surface, and the result is largely similar to the particles depicted in Figure 1. When toluene was replaced by D_4 or the rotation speed was increased using toluene (Table 1, entries 2 and 4), the hollow sphere formation and thus the templating effect were observed as indicated in Figure 3(*b*) for the toluene case and in Figure 3(*d*) for the D_4 one.

The hollow cores have been observed so far typically for the smaller particles derived from little-size droplets. This observation can be regarded as an indication that templating with the fast agglomerating silica particles requires high volume density of the template droplets. Measurement of the powddensity and specific surface area resulted in values of 0.3 g cm^{-3} and 100 m^2 g^{-1}, respectively, for Table 1, entry 5 using D_4 at 5×10^3 rpm. Compared with the bulk density of amorphous silica, which we have determined to be 1.58 g cm^{-3}, these data are in agreement with the formation of large fraction of cavities. As followed from the

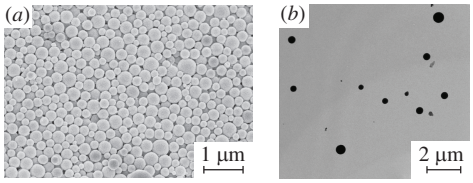

Figure 2 Particles obtained by addition of molecular silica sol to the toluene-in-water emulsion at 2×10^3 rpm (Table 1, entry 1). Average size of the particles was 440 nm, no hollow core was detected by TEM.

Table 1 Particles prepared by dispersing silica sol into oil–water emulsion.

Entry	Disperse phase	Rotation speed (rpm)	Solid spheres	Hollow spheres	Particle size[a]/nm	Powder density/ g cm^{-3}	Product yield[b] (%)
1	toluene	2×10^3	+	–	440 ± 150	–	95
2	toluene	5×10^3	+	+	300 ± 200	–	95
3	toluene	1×10^4	–	–	–	–	95
4	D_4	2×10^3	+	+	250 ± 200	–	95
5	D_4	5×10^3	+	+	280 ± 200	0.3[c]	95
6	D_4	1×10^4	–	–	–	–	95
7	D_4[d]	5×10^3	+	+	280 ± 200	–	–

[a] Determined from SEM and TEM images. [b] Relative to silica content in the initial silica sol load. [c] *Cf.* the bulk density of amorphous silica (1.58 g cm^{-3}). [d] D_4 mixed with fluorescent dye (BODIPY-modified PDMS, 0.2 wt% relative to D_4).

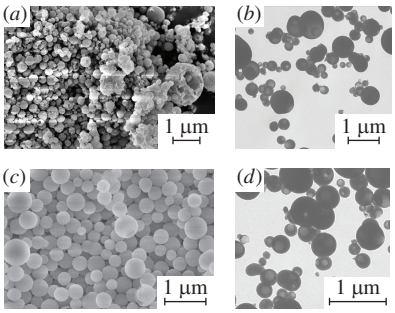

Figure 3 Microscopy images for particles obtained under conditions of Table 1, entry 2: (*a*) SEM and (*b*) TEM as well as entry 4: (*c*) SEM and (*d*) TEM.

FT-IR spectra, the templating oil could be removed completely when the spheres were isolated from an aqueous dispersion using centrifugation. This ease of removal revealed that the shells formed by the silica sol particles still contained micropores as well as small mesopores, through which the oil phase was released. This was confirmed by the confocal micrograph of a hollow silica particles (Figure 4) obtained employing D_4 mixed with BODIPY-modified PDMS, where a rather homogeneous coloration through the spheres was present.

Note that neither solid nor hollow spheres could be observed when the rotation speed was increased further using D_4 or toluene as the template liquid (Table 1, entries 3 and 6), only the irregular agglomerates were detected by electron microscopy.

Taking into account the structure of the silica sol particles comprising hydrophobic as well as hydrophilic surface groups, we explain these results by a two-step consolidation process, where single particles agglomerate to form sphere or to template an oil droplet with generation of a shell around the droplet. In a first step, the ultrasmall particles assemble through noncovalent bonding such as hydrophobic interaction and/or hydrogen bond formation between their silanol groups. This process is fast and relatively instantaneous. Only in a second step the structure is consolidated by covalent bond formation due to condensation of the silanol groups. This process is slow, and an intensive shearing effect at high rotation speeds destroys the initially assembled structure. Since the initial association becomes irreversible, only irregular agglomerates are formed in the aqueous phase.

In summary, we have demonstrated the scope of silica sols with ultrasmall active particles to template the shape of microscopic oil droplets. Most importantly, the particles assemble at the oil–water interface similar to larger colloids but can react with each other at the second condensation step. By choosing neutral conditions (pH 7) for the condensation reaction, this step can be slowed to take significantly more time than the original assembly process. We conclude that the former is mostly controlled by the pre-dispersion and mixing conditions. Compared with the reactive shell formation, the first agglomeration process is much faster and has a potential for undesired coagulation and the Oswald ripening. It can be optimized further as we plan in our investigations.

This work was supported by the Ministry of Science and Higher Education of the Russian Federation (grant of the Government of the Russian Federation no. 14.W03.31.0018). The SEM measurements were performed using the shared experimental facilities supported by the State Assignment of the N. S. Kurnakov Institute of General and Inorganic Chemistry, Russian Academy of Sciences. The authors are grateful to Dr. Yu. N. Kononevich (INEOS RAS) for the provided BODIPY-modified PDMS.

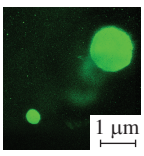

Figure 4 Confocal microscopy image of particles obtained under conditions of Table 1, entry 7.

References

1 A. S. Doumbia, A. Bourmaud, D. Jouannet, T. Falher, F. Orange, R. Retoux, L. Le Pluart and L. Cauret, *Polym. Degrad. Stab.*, 2015, **114**, 146.
2 W. Suthabanditpong, M. Tani, C. Takai, M. Fuji, R. Buntem and T. Shirai, *Adv. Powder Technol.*, 2016, **27**, 454.
3 X. Ouyang, S. Lei, X. Liu, D. Chen and J. Tang, *Polym.-Plast. Technol. Mater.*, 2019, **58**, 1766.
4 P. Patle and A. Agrawal, *J. Therm. Energy Sys.*, 2019, **4**, 41.
5 G. Jian, Y. Xu, L.-C. Lai, C. Wang and M. R. Zachariah, *J. Mater. Chem. A*, 2014, **2**, 4627.
6 H. F. Gangåssæter, B. P. Jelle and S. A. Mofid, *Energy Procedia*, 2017, **122**, 949.
7 S. Ng, B. P. Jelle, L. I. Sandberg, T. Gao and S. A. Mofid, *Constr. Build. Mater.*, 2018, **166**, 72.
8 S. De Koker, R. Hoogenboom and B. G. De Geest, *Chem. Soc. Rev.*, 2012, **41**, 2867.
9 Z. G. Denieva, U. A. Budanova and Yu. L. Sebyakin, *Mendeleev Commun.*, 2019, **29**, 32.
10 J. Hu, M. Chen, X. Fang and L. Wu, *Chem. Soc. Rev.*, 2011, **40**, 5472.
11 S. F. Soares, T. Fernandes, A. L. Daniel-da-Silva and T. Trindade, *Proc. R. Soc. A*, 2019, **475**, 20180677.
12 V. V. Kazakova, A. S. Zhiltsov, O. B. Gorbatsevitch, I. B. Meshkov, M. V. Pletneva, N. V. Demchenko, G. V. Cherkaev and A. M. Muzafarov, *J. Inorg. Organomet. Polym. Mater.*, 2012, **22**, 564.
13 A. Zhiltsov, O. Gritsenko, V. Kazakova, O. Gorbatsevitch, N. Bessonova, A. Askadskii, O. Serenko and A. Muzafarov, *J. Appl. Polym. Sci.*, 2015, **132**, 41894.
14 C. I. Zoldesi, C. A. van Walree and A. Imhof, *Langmuir*, 2006, **22**, 4343.
15 C. I. Zoldesi, P. Steegstra and A. Imhof, *J. Colloid Interface Sci.*, 2007, **308**, 121.
16 M. O'Sullivan, Z. Zhang and B. Vincent, *Langmuir*, 2009, **25**, 7962.
17 H. Wang, G. Agrawal, L. Tsarkova, X. Zhu and M. Möller, *Adv. Mater.*, 2013, **25**, 1017.
18 J.-S. Chang, K. L. B. Chang, D.-F. Hwang and Z.-L. Kong, *Environ. Sci. Technol.*, 2007, **41**, 2064.
19 I. I. Slowing, J. L. Vivero-Escoto, C.-W. Wu and V. S.-Y. Lin, *Adv. Drug Delivery Rev.*, 2008, **60**, 1278.
20 T. G. Terentyeva, A. Matras, W. Van Rossom, J. P. Hill, Q. Ji and K. Ariga, *J. Mater. Chem. B*, 2013, **1**, 3248.
21 D. J. French, A. T. Brown, A. B. Schofield, J. Fowler, P. Taylor and P. S. Clegg, *Sci. Rep.*, 2016, **6**, 31401.
22 R. Aveyard, B. P. Binks and J. H. Clint, *Adv. Colloid Interface Sci.*, 2003, **100–102**, 503.
23 T. Bollhorst, K. Rezwan and M. Maas, *Chem. Soc. Rev.*, 2017, **46**, 2091.
24 A. D. Dinsmore, M. F. Hsu, M. G. Nikolaides, M. Marquez, A. R. Bausch and D. A. Weitz, *Science*, 2002, **298**, 1006.
25 Y. Zhao, Y. Li, D. E. Demco, X. Zhu and M. Möller, *Langmuir*, 2014, **30**, 4253.
26 B. P. Binks and T. S. Horozov, *Angew. Chem., Int. Ed.*, 2005, **44**, 3722.
27 H. Wang, X. Zhu, L. Tsarkova, A. Pich and M. Möller, *ACS Nano*, 2011, **5**, 3937.
28 C. Zhang, C. Hu, Y. Zhao, M. Möller, K. Yan and X. Zhu, *Langmuir*, 2013, **29**, 15457.
29 Y. Zhao, Z. Chen, X. Zhu and M. Möller, *J. Mater. Chem. A*, 2015, **3**, 24428.
30 S. Schacht, Q. Huo, I. G. Voigt-Martin, G. D. Stucky and F. Schüth, *Science*, 1996, **273**, 768.
31 C. E. Fowler, D. Khushalani and S. Mann, *Chem. Commun.*, 2001, 2028.
32 P. T. Tanev and T. J. Pinnavaia, *Science*, 1996, **271**, 1267.
33 B. P. Binks, *Curr. Opin. Colloid Interface Sci.*, 2002, **7**, 21.
34 A. Walther and A. H. E. Müller, *Chem. Rev.*, 2013, **113**, 5194.
35 V. V. Kazakova, E. A. Rebrov, V. B. Myakushev, T. V. Strelkova, A. N. Ozerin, L. A. Ozerina, T. B. Chenskaya, S. S. Sheiko, E. Yu. Sharipov and A. M. Muzafarov, in *Silicones and Silicone-Modified Materials* (*ACS Symposium Series*, vol. 729), eds. S. J. Clarson, J. J. Fitzgerald, M. J. Owen and S. D. Smith, *American Chemical Society*, 2000, pp. 503–515.
36 N. V. Voronina, I. B. Meshkov, V. D. Myakushev, T. V. Laptinskaya, V. S. Papkov, M. I. Buzin, M. N. Il'ina, A. N. Ozerin and A. M. Muzafarov, *J. Polym. Sci., Part A: Polym. Chem.*, 2010, **48**, 4310.

Received: 21st April 2020; Com. 20/6202